Progress In Electromagnetics Research C, Vol. 14, 213–225, 2010

DUAL BAND-NOTCHED DESIGN OF RECTANGULAR MONOPOLE ANTENNA FOR UWB APPLICATIONS

C. Deng and Y. J. Xie †

National Laboratory of Antennas and Microwave Technology
Xidian University
P. O. Box 223, Xi'an, Shannxi 710071, China

J. F. Yuan

Engineering College of Chinese Armed Police Force
Xi'an, Shannxi 710086, China

Abstract—An ultra wideband (UWB) coplanar waveguide (CPW) fed rectangular monopole antenna, which is of band notched characteristic for Wireless Local Area Network (WLAN), Worldwide inter-operability for Microwave Access (WiMAX) and the C-band satellite communications, is proposed, fabricated and measured. In order to obtain the desired dual band rejections, a piece of pentagonal slotline and a pair of inverted L-shaped stubs are loaded on the CPW fed rectangular monopole antenna of enhanced impedance bandwidth. The antenna is printed on the FR4 substrate of 40 mm (width) × 41 mm (length) × 0.5 mm (thickness), and is optimized by ANSOFT HFSS. A prototype is fabricated according to the optimized parameters values, and the antenna characteristics are measured. The results show that the antenna is of UWB characteristic and exhibits band rejection of 3.2–4.25 GHz and 5.1–6.15 GHz, which covers WLAN, WiMAX, and C-band satellite communications.

1. INTRODUCTION

Under the extensive demands of various wireless operations, UWB systems usually operate at close quarters with other wireless systems resulting in the intersystem interference. The

Corresponding author: C. Deng (dczq100w@yahoo.cn).
† C. Deng is also with Engineering College of Chinese Armed Police Force, Xi'an, Shannxi 710086, China; Y. J. Xie is also with EMC Laboratory, Beihang University, Beijing 100191, China.

frequency band allocated for UWB communications is 3.1–10.6 GHz. The typical existing narrow-band systems within this frequency band are WLAN (2.4–2.484 GHz/5.15–5.35 GHz/5.725–5.85 GHz), WiMAX (2.5–2.69 GHz/3.3–3.8 GHz/5.25–5.85 GHz), and C-band satellite communications (3.8–4.2 GHz). In order to achieve compatibility among the different wireless systems and make the best use of the electromagnetic spectrum, much research of interference suppression has been reported in recent years. Among all of the existing schemes, the antenna of band-rejected characteristic is deemed as one of the most effective methods. Therefore, such antennas are attention-getting in antenna topics.

The design methods of band-rejected antennas mainly include two types, which are, respectively, integrating a filter at the input end of the antenna [1] and loading narrow-band resonant elements on the antenna [2]. Although the filter integration can endow antennas with band-rejected function, they are large in size and complicated in structure. Therefore, antennas of the latter type are preferred in the practical applications. Its design principle is to make a remarkable variation of the antenna input impedance within the desired frequency band. Little energy is therefore radiated or received as the result of the serious input reflection. The loaded narrow-band resonators usually take the forms of slotline [3], strip [4, 5], SRR [6], CSRR [7], fractality [8], etc. Their positions mainly locate where the electrical field is relatively strong, such as on the radiator [9], on the ground [10] or around the feed line [11]. Single band-rejected function can be realized by one resonator, while two or more resonators are usually needed for multi-band notch. Most of the research before concentrated on the antennas with single band-rejected characteristic, and some aimed at the multi-band-rejections. However, report on the rejections at the entire frequency bands of WLAN, WiMAX and C-band satellite applications was rare. Actually, with the increasing complications in the electromagnetic circumstance of the UWB communications, the disturbances of various wireless narrow-band systems to them are noticeable. It is necessary to design an antenna with rejected bands at 3.3–4.2 GHz and 5.15–5.825 GHz.

The band notched characteristic of a new CPW fed rectangular monopole antenna is researched in this paper. Based on the optimized configuration of the antenna with UWB characteristic, a piece of pentagonal slotline is loaded near the feed area at the patch bottom to render the band rejection of 5.15–5.85 GHz. Furthermore, according to the current distributions on the rectangular patch, a pair of inverted L-shaped stubs is loaded at the patch edges to notch the frequency bands of 3.3–4.2 GHz. The impedance and radiation characteristics of the antenna with dual band rejection were simulated and measured. The detailed discussions are presented in this paper.

2. ANTENNA CONFIGURATION

2.1. Conventional UWB Antenna

In [12], we proposed an improved CPW fed rectangular monopole antenna, whose profile is shown in Fig. 1. The rectangular patch and the CPW are printed on the same side of the FR4 substrate with $\varepsilon_r = 4.4$ and thickness $t = 0.5$ mm. The CPW line is of $50\,\Omega$ characteristic impedance with $w_c = 2.8$ mm and $g_c = 0.2$ mm. An M-shaped notch of a (width) $\times$ b (length) is notched at the patch bottom. The CPW ground in the notch presents T-shaped configuration. The edges of the rest CPW ground follow exponential regularity of $y = e^{\beta z} + \gamma$. The UWB characteristic of the antenna is obtained by the tapered CPW ground edges and the tapered slotline between the T-shaped ground and the top of the M-shaped notch.

The relation between the length l and width w of the rectangular patch is given by [13]

$$f_l = 72/[(l + r + p) \times k] \tag{1}$$

where l is the length of the equivalent cylindrical monopole (which is equal to the length of the rectangular patch in this circumstance), r is the effective radius of an equivalent cylindrical monopole antenna

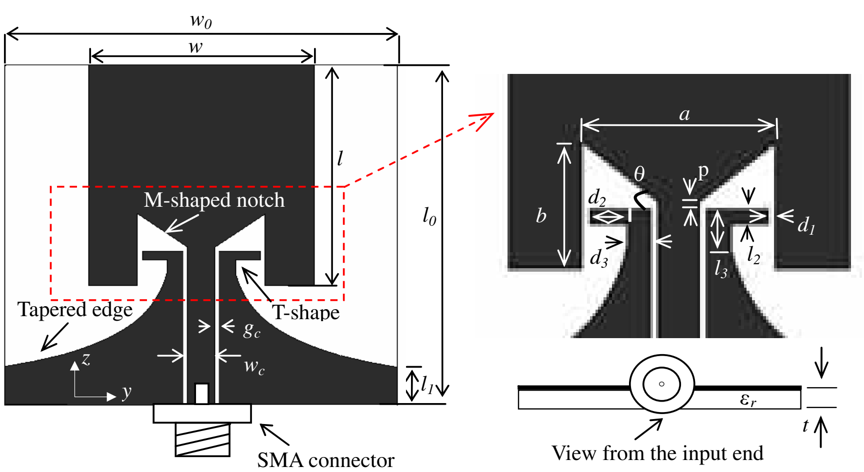

Figure 1. Profile of the conventional UWB antenna.

(given by $r = w/(2 \times \pi)$), p is the length of the feed line. All of the above three parameters in the equation are in millimeter. The empirical value of k was reported as 1.1 for a dielectric substrate with $\varepsilon_r = 4.4$. Given $p = 0.5$ mm and $f_l = 2.1$ GHz, Equation (1) is equal to

$$l + 0.16w = 30.7 \tag{2}$$

Equation (2) gives the approximate relationship between l and w when the antenna renders a low cut-off frequency of 2.1 GHz for VSWR = 2.0. Based on Equation (2), HFSS was adopted to simulate and optimize the rectangular patch. The configurations of the M-shaped notch, T-shaped ground and tapered rate of the ground edges were also optimized for UWB characteristic of the antenna. The optimization follows the procedure presented in [12]. Table 1 gives the optimal values of the antenna parameters. It is notable here that Equations (1) and (2) suppose the CPW ground is big enough. Actually, the sizes of the substrate, on which the patch and the CPW are printed, are usually limited in practical applications. The impact of the ground size on the low-cutoff frequency was researched by varying the values of w_0 in Fig. 1. The parameters values in Table 1, except w_0 and l_1, were set to be constant during this procedure. Fig. 2 shows the antenna VSWR curves at low frequency band for different values of w_0. It can be seen that the low-cutoff frequency reduces from 2.27 to 2.1 GHz with w_0 increasing from 30 to 45 mm.

Table 1. Optimized parameters of the conventional UWB antenna (Unit: mm).

a	b	d_1	d_2	d_3	l_0	l	l_1	l_2	l_3	w_0	w	β	γ	θ
12.8	6.1	0.5	2.5	1.9	41	26.6	4.6	1.1	1.6	40	23	−0.3	2.5	20.6°

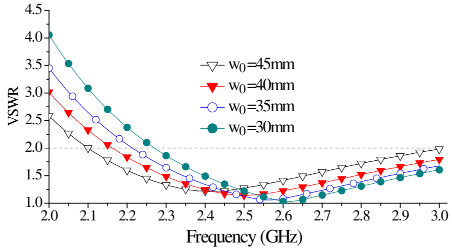

Figure 2. VSWR curves versus frequency for different w_0.

2.2. Proposed UWB Antenna

The proposed antenna of dual band notched characteristic is designed based on the configuration of the conventional UWB antenna with the optimal parameters values in Table 1. Its configuration is shown in Fig. 3(a). As we discussed in [12], the current distributions of the conventional antenna concentrate around the tapered slotline and the two sides of the rectangular patch. According to the current distributions, a piece of pentagonal slotline is loaded near the tapered slotline to render a band rejection. Furthermore, in order to obtain the other band rejection, a pair of inverted L-shaped stubs is loaded at the two sides of the patch. The dual band rejections are achieved by the narrow band resonant characteristic of the two types of elements. In order to further interpret the adopted band notch technique, the

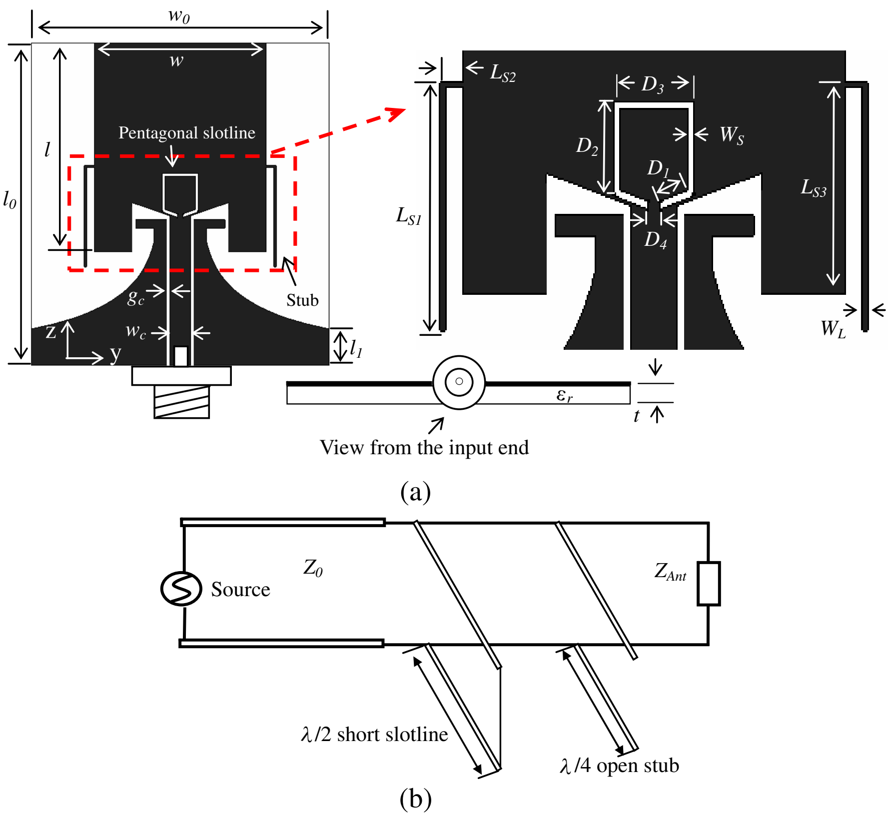

Figure 3. Proposed antenna. (a) Configuration. (b) Equivalent transmission line model.

equivalent transmission line model of the proposed antenna is shown in Fig. 3(b). Supposing the resonant frequencies of the short slotline and the open stub are, respectively, f_1 and f_2, we can conclude the circuit is shorted when $f = f_1$ or f_2, since the lengths of the slotline and the stub are $\lambda_1/2$ and $\lambda_2/4$, respectively. According to the above analysis, the band-rejected characteristic of the proposed UWB antenna depends on the parameters of the loaded elements, such as the positions, the total length, and the length of each segment, etc. The total length of the slotline and the stub, respectively, follow the equations:

$$L_{slot} = 2(D_1 + D_2 + D_3/2) \approx \frac{c}{2f_1\sqrt{(\varepsilon_r + 1)/2}} \tag{3}$$

$$L_{stub} = (L_{s1} + L_{s2}) \approx \frac{c}{4f_2\sqrt{(\varepsilon_r + 1)/2}} \tag{4}$$

where c and ε_r, respectively, denote the speed of the light in the free space and the relative permittivity of the substrate.

Based on Equations (3) and (4), the parameters of the loaded elements were simulated and optimized with HFSS for the desired dual frequency band notch. The rectangular patch and CPW adopted in the proposed antenna are of the same dimensions with the conventional one in Fig. 1. The optimized procedure in this section of simulations aims at the parameters of the loaded elements, such as the loaded positions, the total lengths and each segmental length. A set of optimal parameters values of the loaded elements is given in Table 2. Fig. 4 plots the simulated reflection coefficient curves of the proposed UWB

Table 2. Optimized parameter values of the loaded elements (Unit: mm).

D_1	D_2	D_3	D_4	L_{S1}	L_{S2}	L_{S3}	W_L	W_S
2.1	4.7	4.5	0.7	12.9	1.4	11	0.3	0.2

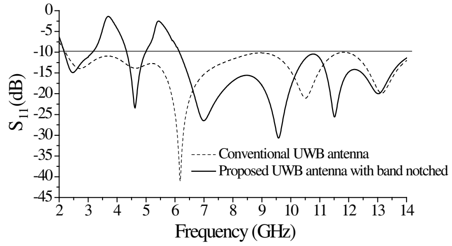

Figure 4. Simulated S_{11} curves of the proposed and conventional antennas.

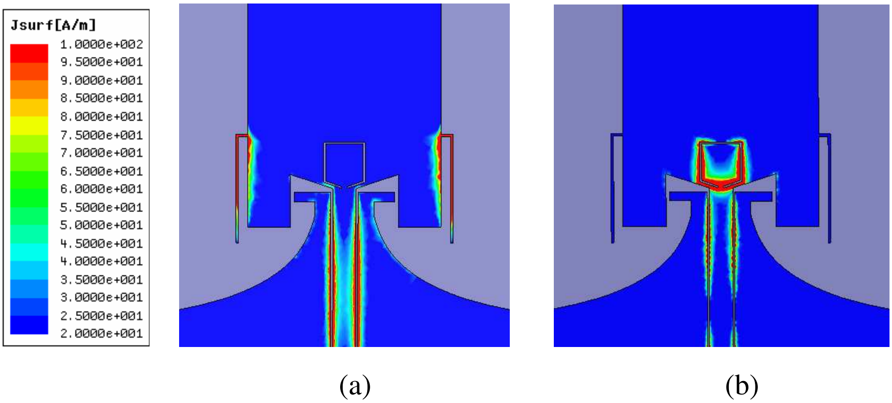

Figure 5. Current distributions. (a) At 3.7 GHz. (b) At 5.5 GHz.

antenna with dual band notched. The S_{11} curve of the conventional UWB antenna is also plotted in this figure for comparison. The simulated reflection coefficient of the proposed antenna is more than -10 dB in the frequency bands of 3.16–4.33 GHz and 5–6.15 GHz, and is better than -10 dB in the rest bands. The simulated result shows the proposed antenna is of good band notched characteristic in the desired frequency bands covering WLAN, WiMAX and the C-band satellite communication systems. It is also seen from the results that the Bluetooth applications at 2.4 GHz is covered by the new antenna. Figs. 5(a) and (b) shows the current distributions on the antenna surface at 3.7 GHz and 5.5 GHz, respectively. It can be seen that the surface current concentrate on the inverted-L shaped stubs at 3.7 GHz and around the pentagonal slotline at 5.5 GHz resulting in the rectangular patch radiating little energy around the above two frequencies.

3. RESULTS AND DISCUSSIONS

The dual band notched characteristic of the proposed UWB antenna is realized by the loaded elements of the inverted-L-shaped stubs and the pentagonal slotline. Their impacts on the antenna characteristics are analyzed with HFSS, and the simulated results are discussed in this section. The proposed antenna is fabricated according to the optimized parameters in Tables 1 and 2, and the measured results are also presented.

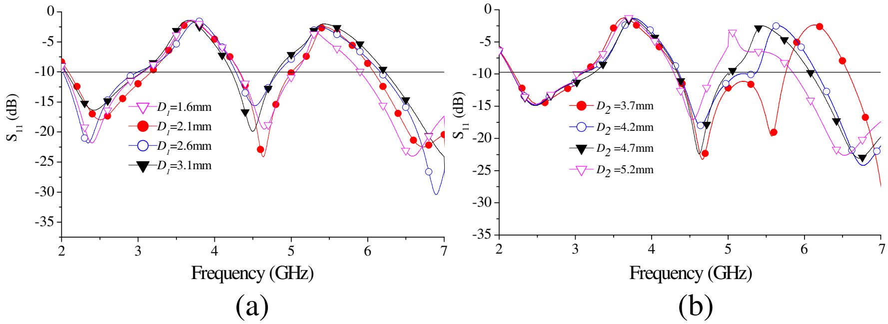

Figure 6. Reflection coefficient curves versus frequency. (a) Different D_1. (b) Different D_2.

3.1. Pentagonal Slotline

According to the center frequency of the band to be rejected, the total length of the pentagonal slotline was firstly evaluated by Equation (3), and then optimized with HFSS. In the optimization procedure, the slotline parameters including the total length and each segmental length were optimized. Fig. 6(a) shows the reflection coefficient curves for different values of D_1 when the total length of the pentagonal slotline and the other parameters in Tables 1 and 2 were set to be constant. We find from the simulations that the notched frequency band reduces from 4.8–6.2 GHz to 5–6 GHz (S_{11} more than -10 dB) with D_1 minimizing from 3.1 mm to 1.6 mm. The impact of the slotline total length on the band notched characteristic of the antenna was also researched by varying the value of D_2 when the other parameters in Tables 1 and 2 were constant. The reflection coefficient curves for different D_2 are plotted in Fig. 6(b). It is found that, with D_2 increasing, the notched frequency band shifts downwards along the frequency axis and the notched frequency bandwidth broadens.

3.2. Inverted L-Shaped Stub

The current distribution on the radiator concentrates around the two lateral edges of the rectangular patch. Accordingly, the stub was designed to be inverted L-shaped. As we can see from Fig. 3(a), the loaded position of the stub along $\hat{z}$ direction depends on the value of L_{S3}, and L_{S2} decides the distance of the stub along $\hat{y}$ direction to the patch edges. Therefore, both L_{S2} and L_{S3} should be considered when studying the loaded position of the stub at the rectangular patch edges. The impacts of the inverted L-shaped stub with different parameters of each segmental length and loaded positions were researched by HFSS. Fig. 7(a) plots the reflection coefficient curves versus frequency for different L_{S1} when the values of the other parameters in Table 1 are constant. We find from the simulation with L_{S1} reducing the center frequency of the notched band caused by the stub moves upwards along the frequency axis while the upper frequency within the notched band is affected slightly. Fig. 7(b) presents the reflection curves for different L_{S2} when the stub total length is 14.3 mm, which is chosen according to each segmental length of L_{S1} and L_{S2} in Table 2. It is found that with L_{S2} increasing the notched frequency bandwidth broadens. The impact of the loaded position of the stub was researched by changing L_{S3}, and the reflection coefficient curves for different L_{S3} are plotted in Fig. 7(c). It can be seen that with L_{S3} increasing the upper frequency of the notched band lowers leading to the reduction of the notched frequency bandwidth.

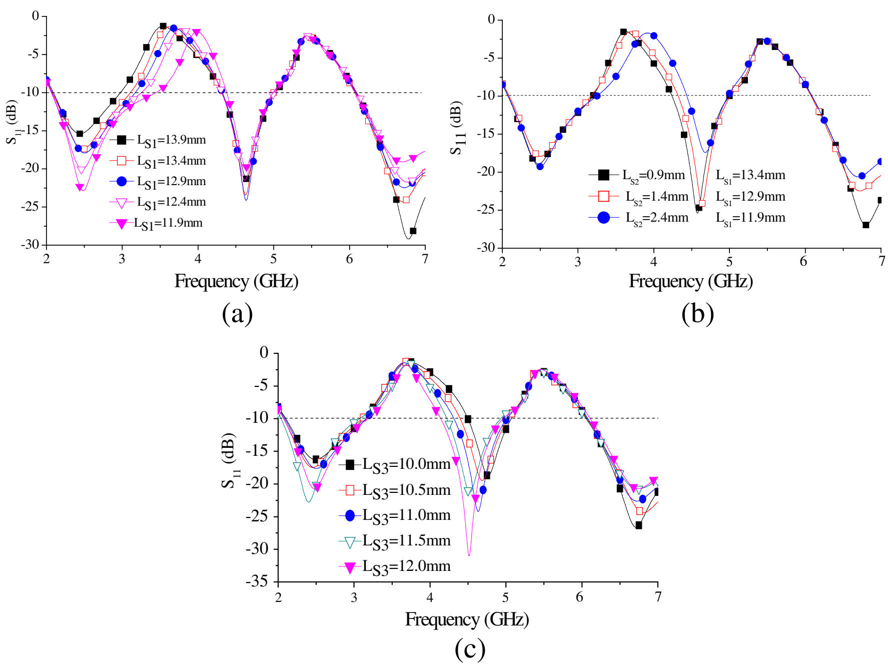

Figure 7. Reflection coefficient curves. (a) For different L_{S1}. (b) For different L_{S2} when the total length of the stub is constant. (c) For different L_{S3}.

3.3. Measured Results

The antenna was fabricated according to the parameters in Tables 1 and 2. Its photograph is shown in Fig. 8. Fig. 9 plots the measured and simulated S_{11} curves versus frequency. We find there is a good agreement between the two curves. The antenna renders dual notched frequency bands of 3.2–4.25 GHz and 5.1–6.15 GHz with measured S_{11} more than -10 dB, and exhibits a good UWB impedance characteristic in the rest frequency bands. Fig. 10 shows the measured antenna gain curves versus frequency. It can be seen that there is a remarkably gain reduction in the notched frequency bands. The antenna radiation patterns were also measured. Figs. 11(a) and (b) give the measured radiation patterns at some given frequencies at the elevation and horizontal planes, respectively.

In order to further test the band notched characteristic of the proposed UWB antenna, the transfer function of the proposed antennas were measured. During the measurement, an identical prototype pair was used as the transmitting and receiving antennas with a separation distance meeting the far field condition. The far field distance for conventional narrow band antennas is given by

$$R = 2D^2/\lambda \tag{5}$$

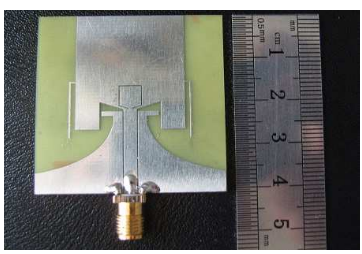

Figure 8. Antenna photograph.

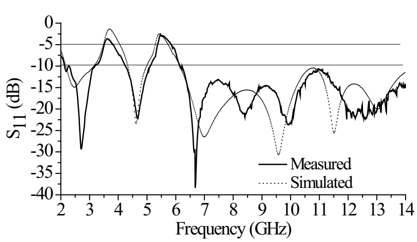

Figure 9. Measured and simulated S_{11} curves.

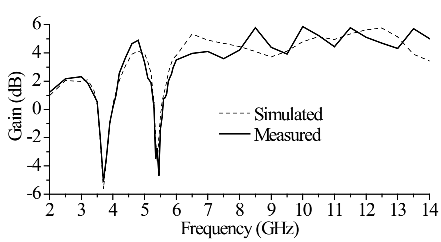

Figure 10. Simulated and measured antenna gain.

where, R is the minimum distance from the center of the radiating source to the far field region at a specific wavelength λ. D is the largest dimension of the antenna. For the proposed antenna in this paper, the largest dimension is about 57.28 mm (diagonal distance of 40 mm $\times$ 41 mm PCB). The measured highest frequency is 14 GHz corresponding to the wavelength of 21.43 mm. According to Equation (5), a minimum separation distance of 30.62 centimeters is therefore needed to meet the far field condition of the proposed antennas. Based on the above calculated value, we chose 35 centimeters as the separation distance of the two antennas in the measurement. Fig. 12 shows the measured amplitude curves of S_{21} versus frequency corresponding to the face-

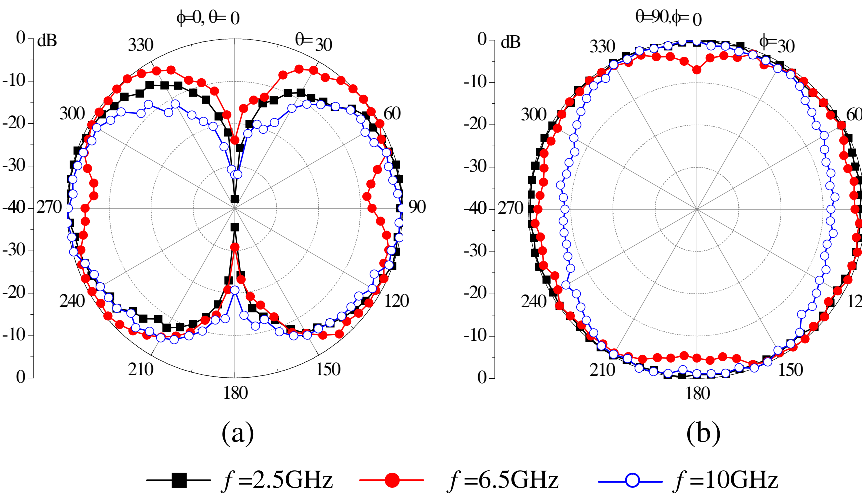

Figure 11. Measured radiation patterns at 2.5, 6.5 and 10 GHz. (a) Elevation radiation patterns; (b) Horizontal radiation patterns.

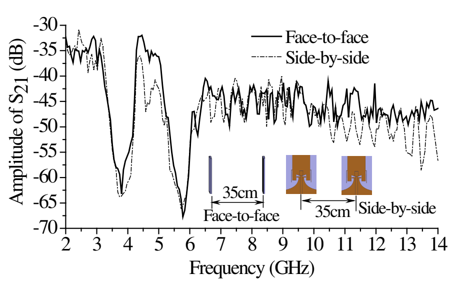

Figure 12. Measured S_{21} curves for different placements of the two proposed antennas.

to-face and side-by-side placements of the two antennas. It can be found there is a rapid reduction of the amplitude of S_{21} in the notched frequency bands.

4. CONCLUSION

In this paper, we studied and designed a piece of UWB rectangular monopole antenna with dual band notched characteristics. Based on the configuration of a CPW fed monopole antenna with impedance bandwidth enhanced, a piece of pentagonal slotline and a pair of inverted L-shaped stubs were loaded on the patch to render a dual band notch. The antenna was simulated with HFSS, and a prototype was fabricated according to the optimal parameters. The antenna characteristics, such as reflection coefficient, radiation patterns and transfer function, were measured. The results show that the antenna has the notched frequency bands of 3.2–4.25 GHz and 5.1–6.15 GHz, which cover WLAN, WiMAX and C-band satellite communications. The proposed antenna is compact in structure and suitable for possible interference suppression in UWB communications.

REFERENCES

1. Yoon, J. K., D. H. Kim, and C. D. Park, "Implementation of UWB antenna with bandpass filter using microstrip-to-CPW transition matching," *Asia Pacific Microwave Conference 2009*, 2553–2556, 2009.
2. Schantz, H. G., G. Wolence, and E. M. Myszka, "Frequency notched UWB antennas," *IEEE Conf. on Ultra Wideband Systems and Technologies*, 214–218, 2003.
3. Barbarino, S. and F. Consoli, "UWB circular slot antenna provided with an inverted-L notch filter for the 5 GHz WLAN band," *Progress In Electromagnetics Research*, Vol. 104, 1–13, 2010.
4. Fallahi, R., A. A. Kalteh, and M. G. Roozbahani, "A novel UWB elliptical slot antenna with band-notched characteristics," *Progress In Electromagnetics Research*, Vol. 82, 127–136, 2008.
5. Zhang, G. M., J. S. Hong, and B. Z. Wang, "Two novel band notched UWB slot antennas FED by microstrip line," *Progress In Electromagnetics Research*, Vol. 78, 209–218, 2008.
6. Ghatak, R., R Debnath, D. R. Poddar, R. K. Mishra, and S. R. B. Chaudhuri, "A CPW fed planar monopole band notched UWB antenna with embedded split ring resonators,"

2009 Loughborough Antennas & Propagation Conference, 645–647, 2009.

7. Weng, Y. F., S. W. Cheung, and T. I. Yuk, "An antenna for UWB and bluetooth standards with band-notched characteristics," *ICUWB 2009*, 170–174, 2009.
8. Falahati, A., M. Naghshvarian-Jahromi, and R. M. Edwards, "Dual band-notch CPW-ground-fed UWB antenna by fractal binary tree slot," *5th International Conference on Wireless and Mobile Communications*, 385–390, 2009.
9. Kim, D. Z. and J. W. Yu, "Wide-band planar monopole antenna with triple band-notched slots," *Journal of Electromagnetic Waves and Applications*, Vol. 23, No. 1, 117–128, 2009.
10. Weng, Y. F., W. J. Lu, S. W. Cheung, and T. L. Yuk, "UWB antenna with single or dual band notched characteristic for WLAN band using meandered ground stubs," *2009 Loughborough Antennas & Propagation Conference*, 757–760, 2009.
11. Halilzadeh, A. K., K. K. M. Chan, and K. Rambabu, "Coupled-line fed dual notch ultra-wideband antenna," *Electronic Letters*, Vol. 46, No. 1, 2010.
12. Deng, C., Y. J. Xie, and P. Li, "CPW-fed planar printed monopole antenna with impedance bandwidth enhanced," *IEEE Antennas and Wireless Propagation Letters*, 2009.
13. Ray, K. P. and Y. Ranga, "Printed rectangular monopole antenna," *Proc. IEEE APS Int. Symp.*, 1636–1639, 2006.